



Bulletin of the Mineral Research and Exploration

<http://bulletin.mta.gov.tr>



Holocene activity of the Orhaneli Fault based on palaeoseismological data, Bursa, NW Anatolia

Volkan ÖZAKSOY^{a*}, Hasan ELMACI^b, Selim ÖZALP^c, Meryem KARA^d and Tamer Y. DUMAN^e

^aAkdeniz University, Faculty of Engineering, Department of Geological Engineering 07058 Konyaaaltı Antalya Turkey. orcid.org/0000-0002-8126-8134.

^bGeneral Directorate of Mineral Research and Exploration, Directorate of Geological Studies, 06800 Çankaya/Ankara. orcid.org/0000-0002-5076-1153.

^cGeneral Directorate of Mineral Research and Exploration, Directorate of Geological Studies, 06800 Çankaya/Ankara. orcid.org/0000-0002-6755-4206.

^dGeneral Directorate of Mineral Research and Exploration, Eastern Mediterranean Regional Directorate 01360 Çukurova/Adana. orcid.org/0000-0002-9143-815X.

^eFugro Sial Earth Sciences Consultancy and Engineering Ltd. 06690 Çankaya/Ankara. orcid.org/0000-0003-3556-2217.

Research Article

Keywords:

Orhaneli fault,
palaeoseismology,
Holocene, Biga Peninsula,
NW Anatolia.

ABSTRACT

Orhaneli Fault is 30 km long, right-lateral strike-slip fault with dominant reverse component located in the Biga Peninsula. This fault controls the southern margin of the Quaternary Orhaneli Basin. Additionally, it cuts the metamorphic rocks of the Tavşanlı Zone, Cretaceous ophiolitic units and Neogene/Quaternary sediments, and can be easily recognized on aerial photographs and in the field due to linearity and fault scarps. Elongated ridges, offset valleys and fault saddles observed along the fault are important geomorphological features indicating fault activity. This study presents the results of the first palaeoseismological study on the Orhaneli Fault. Two trenches were excavated along the fault. These trenches, named Serçeler and Kusumlar, exhibited that metamorphic rocks of the Tavşanlı Zone were thrust onto Quaternary sediments by the fault. The study encountered evidences of four large earthquakes accompanied by surface rupture in Quaternary. The results of Serçeler trench indicated the older earthquake occurred between 22,000±3,200 BC and 6,600±800 BC, and the most recent earthquake occurred before 770-415 BC. The Kusumlar trench data showed that the older earthquake occurred between 6,660 BC and 3,085 BC, and the most recent event in the period after 650 AD. Any interpretation could not be made about the recurrence period between palaeoearthquakes. In this study, Holocene activity on the Orhaneli Fault was proven. If this fault, with 30 km total length comprising two segments, ruptured as a single piece, it has the potential to produce an earthquake with Mw=6.9.

Received Date: 28.05.2017

Accepted Date: 29.09.2017

1. Introduction

Turkey is one of the world's most seismically active country, located within the Alpine-Himalayan Orogenic Belt. The Anatolian platelet is moving westward along the North Anatolian and East Anatolian Faults and rotating in anticlockwise direction due to the northward movement of the Arabian plate (Figure 1A; McKenzie, 1972; Dewey and Şengör, 1979; Şengör et al., 1985). After this orogenesis, neotectonic period began nearly 12 million years ago in the

Middle Miocene (Barka and Hancock, 1984; Şengör et al., 1985) and Anatolia became one of the most seismically active regions in the Eurasian continent. The tectonic escape of the Anatolian platelet linked to the closure between the Arabian and Eurasian plates caused the formation of four neotectonic provinces (Figure 1A) (Şengör et al., 1985). These are (1) the Eastern Anatolian contractional province, (2) the Northern Anatolian strike-slip province, (3) the Central Anatolian "Ova" province and (4) the Western Anatolian extensional province (Şengör et al., 1985).

* Corresponding author: Volkan ÖZAKSOY, volkano@akdeniz.edu.
<http://dx.doi.org/10.19111/bulletinofmre.413248>

The Southern Marmara region, containing the Biga Peninsula, represents a transition zone between the North Anatolian Fault System and the West Anatolian extensional province (Barka, 1992; Barka and Kadinsky-Cade, 1988; Dewey and Şengör, 1979; Emre et al., 2012; Emre et al., 2013; Şaroğlu et al., 1992; Şengör et al., 2005) (Figure 1A, B). The tectonic structures within the South Marmara region are generally represented by right-lateral strike-slip faults, forming a wide arc geometry expanding toward the south (Emre et al., 2011a, b, 2012, 2013) (Figure 1B). The Orhaneli Fault forms the eastern wing of this arc structure together with the Mustafakemalpaşa and Manyas Faults (Emre et al., 2011a, b) (Figure 1B). Orhaneli Fault is first shown as an active, right-lateral strike-slip fault on the Turkish Active Fault Map by Emre et al. (2011a, b, 2013). This study was aimed to prove its Holocene activity as part of the Turkish Palaeoseismology Research Project (TURKPAP). In this palaeoseismological study, structural geology,

sedimentology, geomorphology and radiocarbon/OSL dating methods were applied. It is expected that this study and other previous studies will help to understand the seismicity of the region (Kop et al., 2016; Kürçer et al., 2017; Özalp et al., 2013, 2016; Sözbilir et al., 2016a, b) and the seismic hazard assessment.

2. Regional Geology

The study area is located nearly 60 km south of Bursa (Figure 1B). In the region between Bursa and Orhaneli, there is a large variety of geological units. The most important reason for this variety is that the area contains two tectonic units separated from each other by the İzmir-Ankara Suture Zone (IASZ) (Okay and Tüysüz, 1999). These tectonic units are represented by rocks of Sakarya and Tavşanlı zones. The lithological units observed commonly between Orhaneli and Bursa may be separated into four groups.

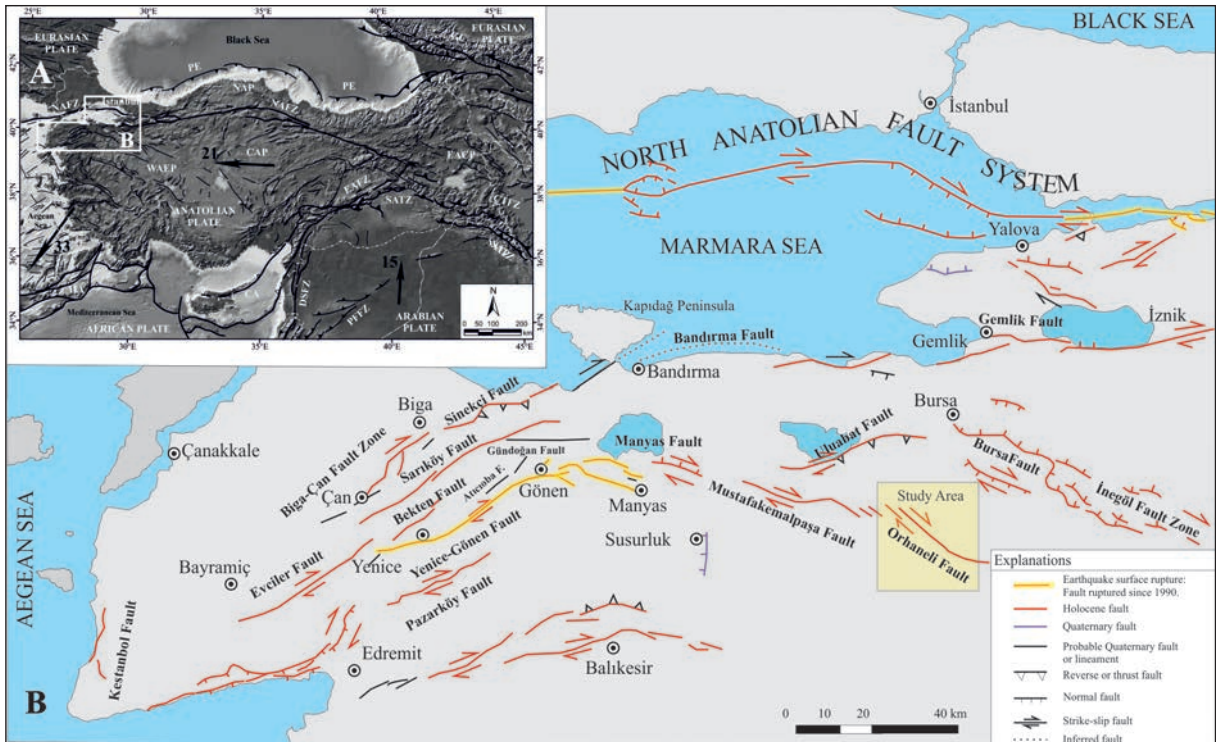


Figure 1- A) Simplified active tectonic map of Turkey and surroundings. Active faults in Turkey taken from Emre et al. (2013), active faults from surrounding area taken from Duman et al. (2016) and references in both. Neotectonic regions taken from Şengör et al. (1985). Subduction zones shown by thick lines and open triangles, with triangles representing the direction of subduction. Thick lines with black filled triangles are thrust faults, black lines with open triangles show reverse faults. Large black arrows indicate the motion rates (mm/yr) for plates compared to the Eurasian Plate (calculated from GPS) (Reilinger et al., 2006). AA: Aegean Arc, CY: Cypriot Arc, DSFZ: Dead Sea Fault Zone, EAFZ: East Anatolian Fault Zone, NAFZ: North Anatolian Fault Zone, SEATZ: South East Anatolian Thrust Zone, WAER: West Anatolian Extensional Region, CAR: Central Anatolian Region, EACR: East Anatolian Compression Region, NAR: North Anatolian Region, PFCZ: Palmira Fault Curve Zone. GeoMap Application data used for digital elevation model. B) Active fault map for the Marmara Region and the study area (adapted from Emre et al., 2013).

- North of the IASZ, rocks from the Sakarya Zone with ages ranging from Palaeozoic to Cretaceous.
- Ophiolitic rocks from the northern branch of the Neotethys Ocean
- Metamorphic and granitic rocks of Tavşanlı Zone south of the IASZ belonging to the Anatolide-Tauride Block
- Sedimentary and volcanic rocks overlying or cutting these units of Miocene and younger ages.

The rocks outcropping and forming the basement in the area of the Orhaneli Fault belong to the Tavşanlı Zone. These were formed by burial to more than 60 km long and blueschist facies metamorphism on the northern edge of the Anatolide-Tauride Block linked to ophiolite obduction in the Late Cretaceous (Okay et al., 1998). The blueschist rocks commonly observed in the Orhaneli region are mainly represented by mica schist, phyllite and metabasites and are called the

Orhaneli Group (Okay, 1985) (Figure 2). The Triassic metamorphic series at the base of the Orhaneli Group is represented by mica schists called the Kocasu formation (Okay, 2004). Kocasu formation is overlain by a marble series with kilometres of thickness. This marble was first called the İnönü Marble by Servais (1982) and is represented by white-grey coloured, occasionally banded carbonates. The age of this formation varies from Late Triassic to Cretaceous (Kaya et al., 2001).

Ophiolitic rocks (Burhan Ophiolite) are commonly observed north and south of Orhaneli and mainly represented by peridotite, gabbro, pyroxenite and diabase (Okay et al., 1998). The Burhan Ophiolite represents mantle and lower crust of Tethys oceanic lithosphere and is reported to have been emplaced on the Anatolide-Tauride platform in the Late Cretaceous (Okay et al., 1998; Okay, 2011). These rocks are tectonically located above the units of Tavşanlı Zone. These units are also cut by the Early Eocene Orhaneli Granodiorite (Harris et al., 1994) (Figure 2).

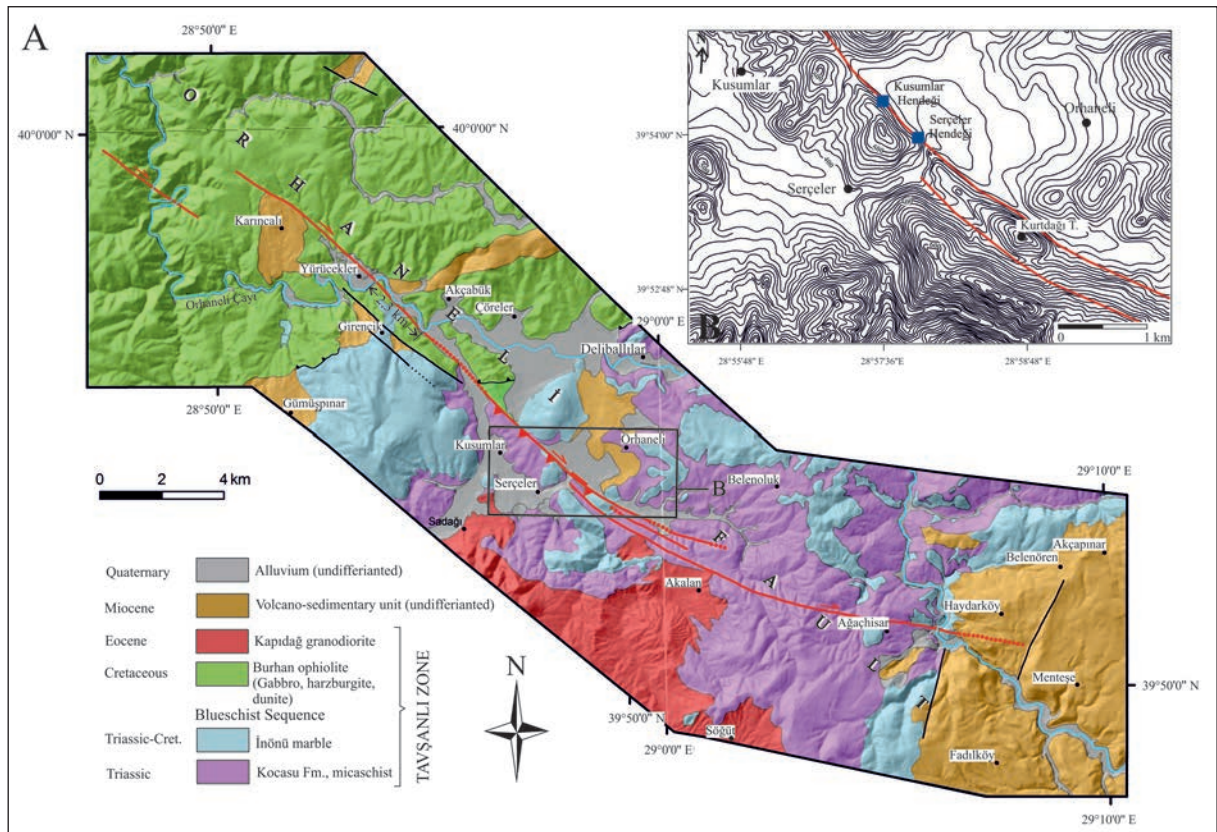


Figure 2- A) Geologic map of Orhaneli Fault and close surroundings (Map: adapted from Konak (2002), Türkcen and Yurtsever (2002) and MTA digital database; Stratigraphy: taken from Okay et al. (1998). B) Fault morphology and trench locations.

Neogene-Quaternary sediments unconformably overlie both the ophiolitic rocks and the rocks belonging to the Tavşanlı Zone (Figure 2). Neogene units are generally represented by sedimentary rocks deposited in lacustrine and fluvial facies, containing occasional lignite beds with economic importance. Quaternary units outcrop in a broad area south of Orhaneli. The Quaternary sediments generally comprise fluvial, floodplain and slope debris.

3. General Characteristics of Orhaneli Fault

Orhaneli Fault located in the South Marmara Region forms the eastern limb of the Manyas Bend together with the Mustafakemalpaşa Fault (Emre et al., 2011a, b) (Figure 1B). The geological fault was first shown on a geological map after work by Okay et al. (1998) though its character was undetermined. This fault as active fault was first named by Emre et al. (2011, 2013) and is shown on the Turkish Active Fault Map (Figure 1B).

The Orhaneli Fault has NW-SE orientation and 30 km length on the revised Turkish Active Fault Map (Emre et al., 2013). The southeast section of the fault between Menteşe and Akalan villages has N80°W orientation, making a slight bend to the northwest with N50°W orientation and ends near Karıncalı village in the NW (Figure 2A).

The fault comprises two geometrically separated segments (Figure 2A). These are the 19 km-long NW segment south of Orhaneli which links with a right extensional stepover to the 13 km-long second segment in the SE. In this section, both segments overlap each other by nearly 1.5 km (Figure 2A). In the NW, the fault links to Mustafakemalpaşa Fault with a series of right-lateral faults varying in length from 4 to 5 km within a zone of 11 km wide (Emre et al., 2011a, b) (Figure 1B and 2A).

The most significant data related to Quaternary activity of the Orhaneli Fault is a 2.3 km of right-lateral offset observed in Orhaneli stream (Figure 2A,

B). Further northwest, the same stream is similarly identified to have 2.5 km of right lateral offset due to the Mustafakemalpaşa Fault (Emre et al., 2011b).

In terms of morphology, the fault is clearly observed on aerial photographs and in the field due to continuous lineament and fault scarps, especially in the section north of Yürücekler and Serçeler villages. Nearly 2 km east of Serçeler village, the long axis of Kurtdağı Hill has an elongated ridge appearance parallel to the strike of the fault (Figure 2B).

4. Seismicity in the Historical and Instrumental Periods

The devastated earthquakes occurring in South Marmara region in the historical period (<1900) appear to be distributed along and around active faults north of the study area (Table 1 and Figure 3). There is no historical earthquake record related to the Orhaneli Fault in the historical period. Additionally historical earthquakes occurred in Mustafakemalpaşa in 1850 and 1851 appear to be the closest historical earthquakes to the Orhaneli Fault (Table 1).

When earthquake records of the instrumental period (1900-2012) (Kadirioğlu et al., 2016) are considered, small and moderate magnitude earthquake activity is observed in the surrounding area (Figure 3). There is not any earthquake activity on the Orhaneli Fault. However, in the vicinity with left step-over structure between Mustafakemalpaşa Fault in the west, there is earthquake activity with magnitude less than 5. In the east, in the section between Orhaneli and Oylat Faults, especially around Domanıç, the density of earthquakes with moderate magnitude varying between 5 and 6 is noteworthy. According to instrumental period records, the largest earthquake occurred in the region is the 6 October 1964 Manyas Earthquake (Ms: 6.9).

Table 1- Historical period earthquake record from the South Marmara Region (modified from Tan et al., 2008). References in the table: a) Ergin et al., 1967; b) Ergin et al., 1971; c) Soysal et al., 1981; d) Ambraseys and Finkel, 1991; e) Ambraseys and Jackson, 1998; f) Kondorskaya and Ulomov, 1999; g) Ambraseys and Jackson, 2000; h) Ambraseys, 2002.

No	Date	Coordinates		Magnitude (M)	Intensity (Io)	Location	References*
		Latitude (N)	Longitude (E)				
1	24.11.29	40.50	28.90	6.3	IX	İzmit, İzmit	a
2	? .2.30	40.50	29.50	6.6	?	İzmit-Yalova	f
3	10.11.117	40.40	27.80	7.0	VII	Erdek, Kapıdağ Yarımadası	c, d, h
4	03.05.170	40.10	28.00	6.6	IX	Bandırma, Erdek	a, c
5	02.12.362	40.42	29.72	6.9	IX	İzmit	a
6	11.10.368	40.42	29.72	6.9	VII	İzmit	c, d, e, h
7	? .11.368	40.10	27.80	6.8	VIII	M. Kemalpaşa	c, d, h
8	07.04.460	40.39	27.80	6.9	?	Cyzicus (Erdek)	a, d, e, h
9	? .2.464	40.40	27.85	7.4	VIII	Cyzicus (Erdek), Bandırma	a, c
10	06.09.543	40.39	27.80	6.9	IX-X	Cyzicus (Erdek)-Bandırma?	a, c, d
11	23.09.1064	40.40	28.90	6.9	IX	İzmit, Bandırma, Cyzicus (Erdek)	a, c, h
12	26.11.1143	40.18	29.06	6.0	?	Bursa	B
13	15.03.1419	40.50 40.40	30.50 29.30 (h)	7.0<Ms<7.8 7.2 (h)	?	Geyve ? Bursa (h)	e, h
14	10.05.1556	40.30	27.80	7.2	VIII	Erdek, Edincik	a, d, g, h
15	? .2.1674	40.18	29.10	6.0	?	Bursa	a, c
16	25.05.1719	40.70	29.80	7.4	?	İzmit	g
17	19.04.1850	40.10	28.30	6.1	?	Mustafakemalpaşa	g
18	? .2.1851	40.03	28.40	6.0	?	Mustafakemalpaşa	f
19	28.02.1855	40.00	28.50	7.4	?	Ulubat	e
20	11.04.1855	40.20	29.10 (c)	6.6 (e)	X (e)	Bursa	c, d, e

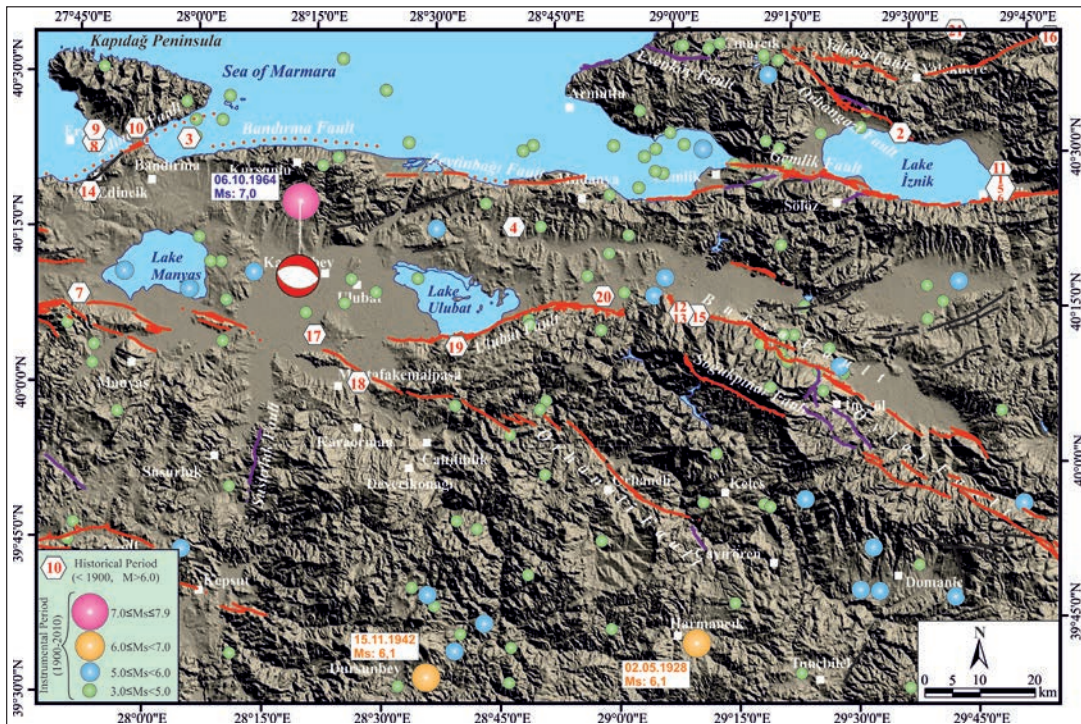


Figure 3- Earthquakes from the historical (see Table 1) and instrumental periods (Kadiroğlu et al., 2016) on the Active Fault Map (Emre et al., 2013). Solution of the 1964 Manyas Earthquake taken from Taymaz et al. (1991).

5. Palaeoseismological Studies

Before palaeoseismological trench studies, aerial photograph analysis of 1: 35.000 scale photographs and later field studies of appropriate areas for excavation determined on aerial photographs were carried out. In the field, there was no data found about surface rupture morphology. As a result, in areas determined by aerial photograph and field studies, geomorphological structures related to Holocene activity were assessed. In the 1 to 2 km section of the Orhaneli Fault between Kusumlar and Serçeler villages, fault morphology is clearly observed (Figures 2 and 4). Therefore, the

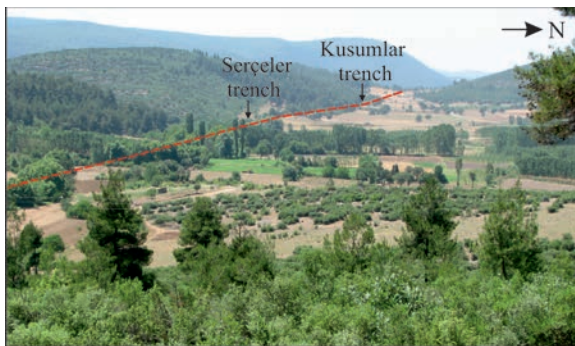


Figure 4- Trench locations, fault scarps and topographic saddle structure of the Orhaneli Fault (looking SW).

boundary between Quaternary basin and metamorphic bedrocks belonging to the Tavşanlı Zone outcropping in the southwest Orhaneli was chosen as the target site for excavation (Figure 2 and 4).

In two different areas along the Orhaneli Fault, trenches were opened perpendicular to the fault with depth from 3 to 3.5 metres. The trench walls were gridded at one metre intervals in horizontal and vertical directions, and detailed cross-section drawings made to determine the stratigraphy of the trench walls. Using tectono-stratigraphic relations, the earthquake horizons were defined. To clearly understand the stratigraphy of the trenches and the earthquake horizons, samples of charcoal and organic materials were taken from stratigraphic units in the trench walls. These samples were dated with the AMS - ^{14}C (radiocarbon) method at BETA Analytic Laboratory in Miami (Florida, USA) (Table 2). Additionally, from some units where AMS - ^{14}C samples could not be found, OSL (optically stimulated luminescence) samples were taken and age dating was performed at the Nuclear Sciences Institute of Ankara University (Table 3).

Table 2- Radiocarbon ages (^{14}C) obtained from Serçeler and Kusumlar trenches.

Sample No	Laboratory No (BETA)	Stratigraphic Unit	Sample Material	Measured Radiocarbon Age (BP)	$\delta^{13}\text{C}$ (‰)	Corrected radiocarbon Age (BP)	Corrected Age (2σ)
SERÇELER TRENCH							
OSCNW-01	390691	Unit 7	Organic Sediment	2530±30	-28,5	2470±30	BC 770 - 415
KUSUMLAR TRENCH							
OK2-C-E01	390692	Unit 6	Coal Sediment	1220±30	-23,9	1240±30	AD 680 - 880
OK2-C-W02	390693	Unit 6	Organic Sediment	NA	NA	1670±30	AD 265 - 275 330 - 420
OK2-C-W06	390694	Unit 6	Organic Material	1340±30	-22,9	1370±30	AD 640 - 675
OK2-C-W08	390695	Unit 6	Coal Sediment	1290±30	-24,3	1300±30	AD 660 - 770
OK2-C-W09	390696	Unit 5	Coal Sediment	4380±30	-26,3	4360±30	BC 3085- 3065

Table 3- OSL (Optically Stimulated Luminescence) ages obtained from Serçeler and Kusumlar trenches.

Sample No.	Stratigraphic Unit	Depth (m)	Conjugate dose (Gy)	OSL age (1000 yrs)
OSRLONW-02	Unit 3	0,70	76,3 ± 8,9	24,0 ± 3,2
OSRLONW-03	Unit 4	0,43	28,3 ± 2,2	8,7 ± 0,8
OSRLONW-05	Unit 2	1,95	133,4 ± 12,2	79,7 ± 9,2
OKSLONW-06	Unit 3a	0,72	33,5 ± 4,9	11,6 ± 1,8
OK2-O-W02	Unit 3b	2,55	27,4 ± 1,8	8,6 ± 1,2

5.1. Serçeler Trench

The trench area was located nearly 1.2 km north of Serçeler village (Figures 2 and 4). The 12 m long, 4 m wide and 3 m deep trench was excavated perpendicular to the fault strike. The trench was opened on the topographic slope break considered to be equivalent to the fault scarp at the boundary between metamorphic rocks of the Tavşanlı Zone and Quaternary sediments (Figures 4 and 5A). Microtopographic mapping was

completed using a total station at 20 cm contour intervals over nearly 15.000 m² area near the excavation site and surroundings (Figure 5B). The fault follows maximum topographic slope break.

The most prominent event in the Serçeler trench is that metamorphic rocks of the bedrock thrust over Quaternary units within the nearly 5 m wide fault zone (Figures 6 and 7). The rake angle of fault striations were generally 70° and higher. As a result,

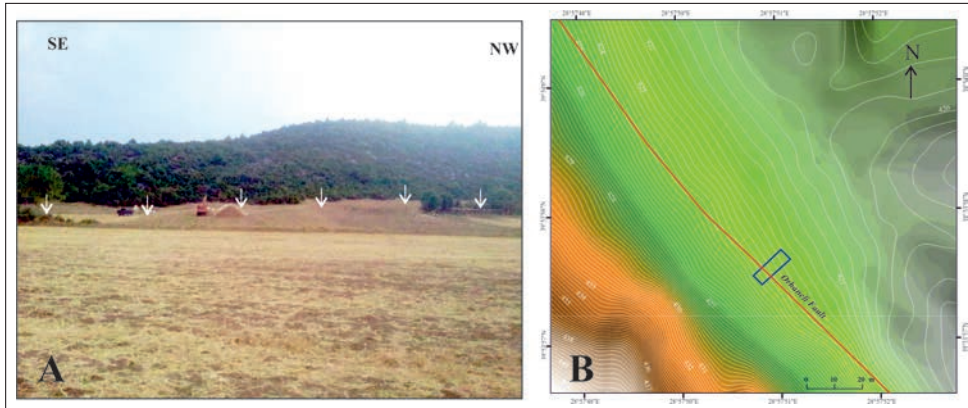


Figure 5- A) Excavation area and fault scarp for Serçeler Trench. White arrows indicate the extension of the fault in the field. B) Microtopographic map of the Serçeler trench area. Contour interval is 20 cm.

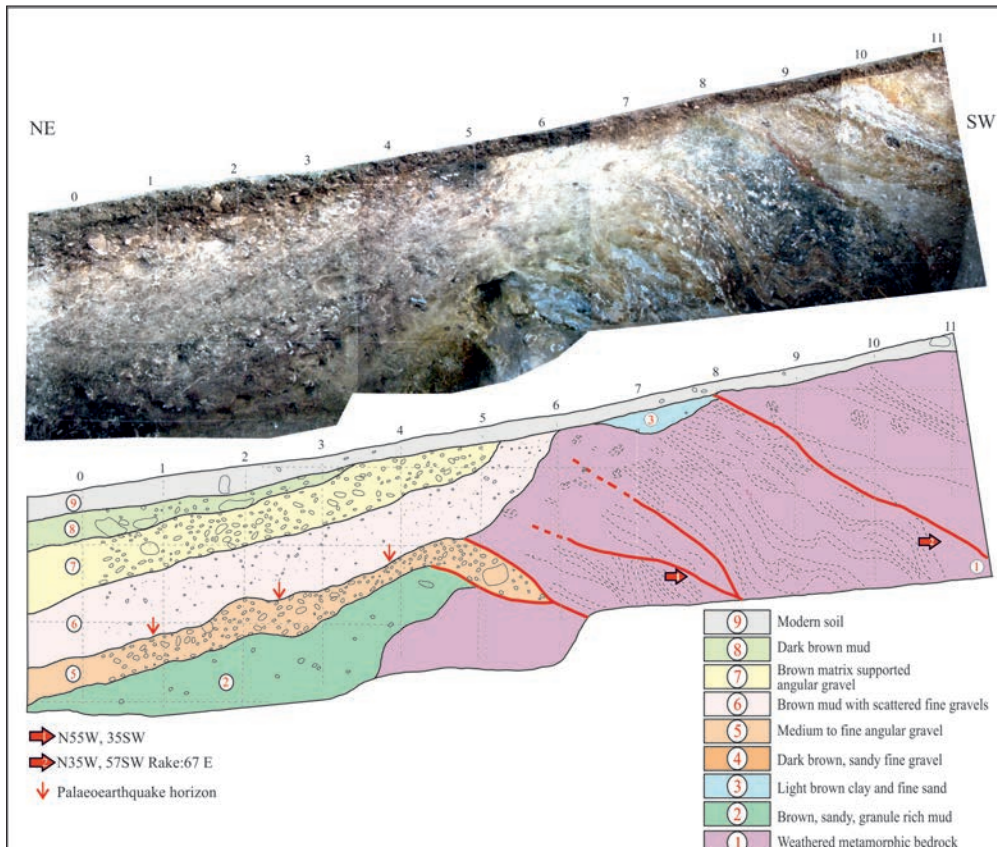


Figure 6- Photomosaic image and interpreted trench log for the SE wall of the Serçeler trench.

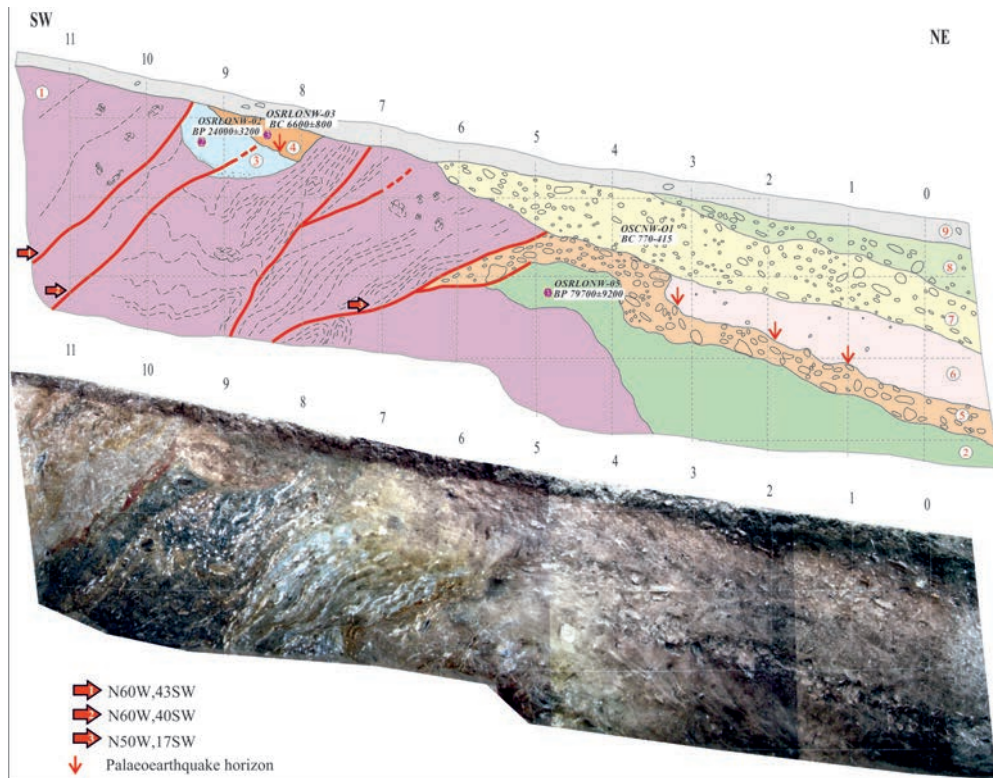


Figure 7- Photomosaic image and interpreted trench log for the NW wall of the Serçeler trench.

in this segment of the Orhanlı Fault where kinematic data may be obtained, the fault has reverse fault character with a right-lateral component (Figure 11). The general strikes of the faults measured in the trench were N50°W, which is in accordance with the strike shown on the Turkish Active Fault Map.

The oldest unit observed in the Serçeler trench is metamorphic bedrock of Tavşanlı Zone, shown on logs as unit 1 (Figures 6 and 7). Primary schistosity can be clearly seen within 4 to 4.5 m wide shear zone despite the intense weathering.

The second stratigraphic unit in the trench is Quaternary sediments. While a part of the sediments overlies unconformably the bedrocks, other part lies below the bedrock units by a series of reverse faults.

Unit 2 is represented by brown, sandy granular mud. It was dated to 79.700±9.200 BP (Before Present) by OSL method (Figure 7 and Table 3). The units 3 and 4 are characterized by gully fill deposits on the bedrock. The 60 cm thick unit is represented by fine pebbles and mud with granules (Figures 6 and 7). The base of this gully (unit 3) is cut and offset by the fault.

Within the same gully fill, unit 4 is not affected by the fault. The OSL samples taken from unit 3 and unit 4 provided ages of 24.000±3.200 BP and 8.700±800 BP, respectively (Figure 7 and Table 3). Unit 5 is represented by angular-semiangular, medium-coarse pebbles. Unit 5 is cut by the fault and overlain by the bedrock. This level, affected by the oldest earthquake was covered by unit 6 after a erosional process.

Unit 7 comprises angular gravels in brownish muddy matrix (Figures 6 and 7). Samples taken from this unit provided a C¹⁴ age of 2530±30 BP (Table 2). This unit is overlain by the dark-brown, blocky, muddy unit 8. All units in the trench are overlain by modern soil level unit 9. This dark brown soil level has mean thickness of 20 cm, with angular pebbles and sandy-muddy composition (Figures 6 and 7).

5.1.1. Palaeoseismological Interpretation

In Serçeler trench, the oldest event in Holocene (or Pleistocene) occurred due to fault observed between 7 and 10^m in the northwest wall. This fault, cutting bedrock units, cuts unit 3 toward the surface and is overlain by unit 4 (Figure 7). The most important

data supporting this event is the presence of colluvial wedge deposits and nearly 15 cm of reverse offset of the gully floor. OSL age of unit 3 containing gully fill sediments cut by the fault is 24.000 ± 3.000 BP. The OSL age of unit 4, interpreted as the earthquake horizon is 6.600 ± 800 BC. As a result, this earthquake must have occurred in the Early Holocene or before, between 24.000 ± 3.200 BP and 6.600 ± 800 BC.

The next earthquake found in Serçeler trench occurred when unit 5 was deformed by the reverse fault-3. Later this unit was covered by unit 7 in the northwest wall (Figures 6 and 7). In the SE wall, this relationship is more clearly observed (Figure 6). Here unit 5 and the fault affected it appear to be overlain by unit no. 6 interpreted as “*earthquake horizon*”. Because age data could not be obtained from unit 6, the closest age data for this earthquake must be before the formation of unit 7, or before 770-415 BC.

5.2. Kusumlar Trench

Kusumlar Trench was excavated nearly 600 m NW of Serçeler trench (Figures 2B and 4). The trench excavated perpendicular to the fault strike is 4 m wide, 3 m deep and 15 m long. As with the Serçeler trench, this trench was opened on the topographic slope break thought to be equivalent of the fault scarp (Figure 8). Kusumlar trench site lies on the boundary between metamorphic basement and Quaternary sediments.

As in Serçeler trench, the basement rocks in this trench were thrust over Quaternary units (Figures 9 and 10). The fault has $N53^{\circ}W$, $23^{\circ}SW$ strike and dip, with rake angles of fault striations reaching $85-90^{\circ}$.

Therefore, the fault is almost a “*pure thrust fault*” in this excavation (Figure 11).

In Kusumlar trench, same as in Serçeler trench, the oldest unit shown as 1 on the log is metamorphic rocks belonging to the Tavşanlı Zone (Figures 9 and 10). Although this unit is highly weathered, primary textures are still visible. The sediments from the Quaternary period observed in the trench were divided into seven stratigraphic units.

Stratigraphically the oldest unit 2 is 1 to 1.5 m thick, coffee-brown, clay sediment rich in pebbles and caliche. Above this, the unit called 3a is represented by light brown, pebbly mud. Unit 3a is 30 cm thick, pinching-out toward the fault zone. The unit marked 3b is whitish-green coloured, weakly layered mud. Above this unit, unit 4 is 20 to 25 cm thick with light brown mud and angular pebble level. The unit 5 is 20-25 cm thick, black mud with angular clasts. The clasts are generally derived from metamorphic basement unit.

After the deposition of these units, the bedrock and sediment fill were experienced an erosional process. The erosional level was covered by unit 6. The apparent thickness of the unit is between 75 and 80 cm, and represented by brown, fine-medium angular pebble-rich mud. This unit displays thickening toward a topographic saddle in NE. The clasts are irregular and disorganised indicating the topographic saddle filled by gravelly mud flow. The sequence in the trench ends with the modern dark-brown soil level of 20 to 25 cm thickness.

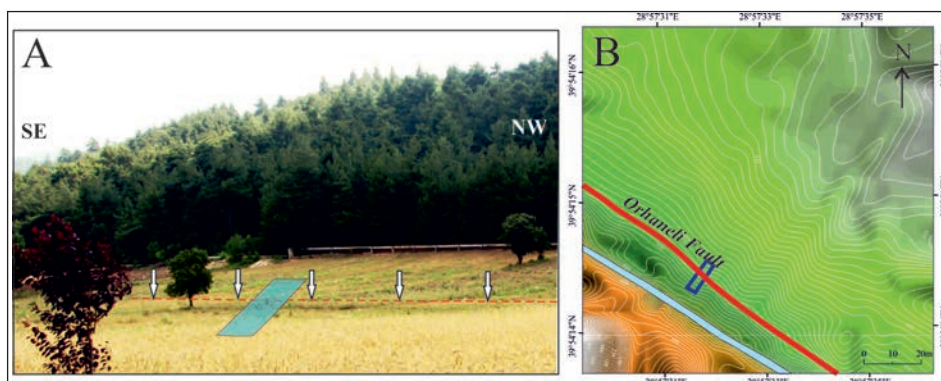


Figure 8- A) General appearance of the area of the Kusumlar trench, white arrows show location of the fault, blue rectangle shows the excavation area. B) Microtopography map of the trench area and close surroundings. Contour interval is 20 cm.

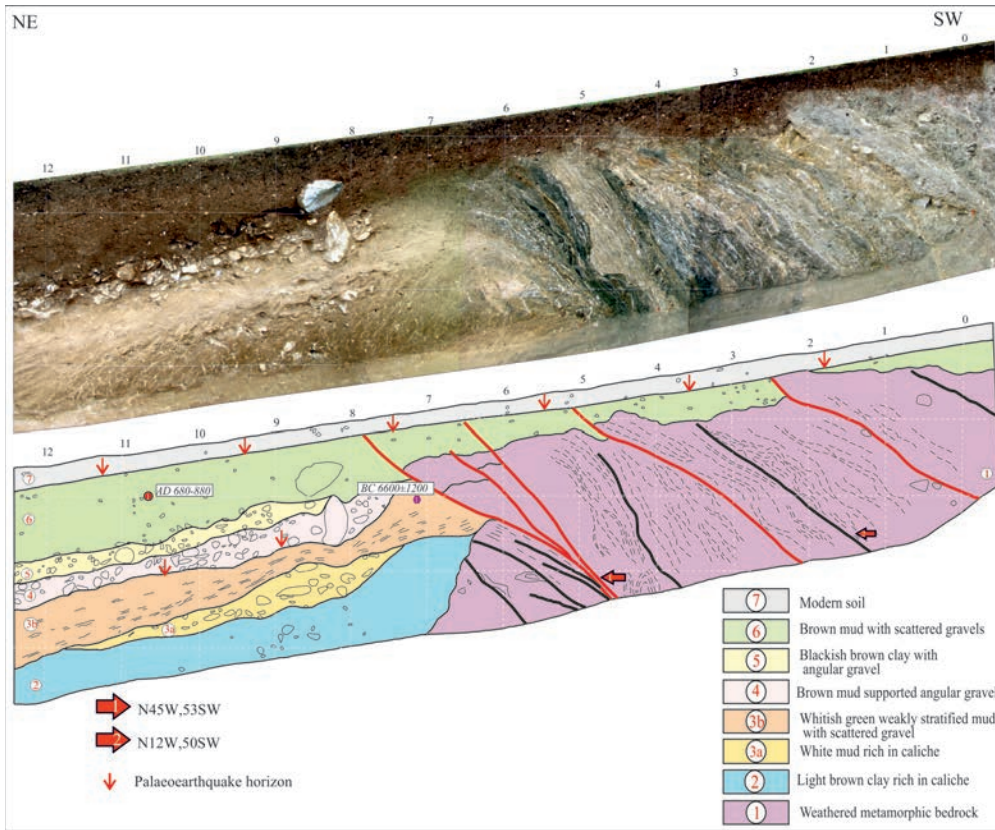


Figure 9- Photomosaic image and interpreted trench log for the SE wall of the Kusumlar trench.

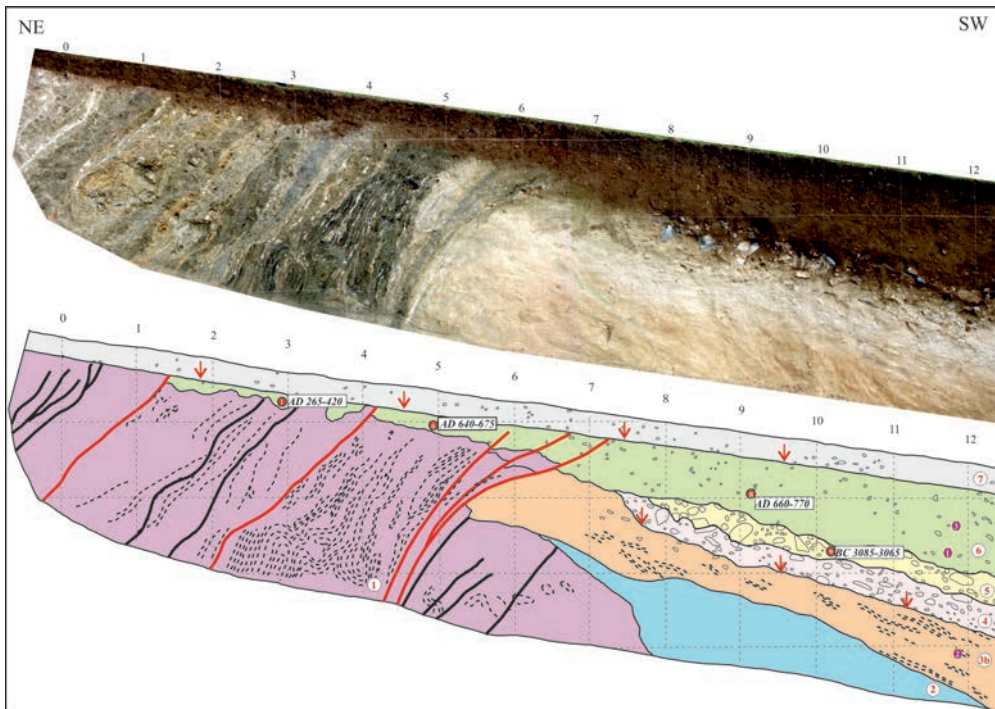


Figure 10- Photomosaic image and interpreted trench log for the NW wall of the Kusumlar trench.

5.2.1. Palaeoseismological Interpretation

The penultimate event in Kusumlar trench occurred by thrusting of the bedrock above unit 3b (Figures 9 and 10). According to an OSL dating of unit 3b, the date is reported as 6.600 ± 1200 BC (Table 3). Among the units overlying it, only unit 5 dated to 3.085-3065 BC based on ^{14}C age. Accordingly, this event (Event-1) must have occurred between 6.600 ± 1200 and 3.065-3085 BC.

Event-2 (last) is characterised by a fault cutting unit 6 and reaching to the base of unit 7 (modern soil level) (Figures 9 and 10). Samples taken from unit 6 reported a mean ^{14}C age of 660-770 AD (Table 2). As a result, Event-2 must have occurred after 660-770 AD.

5.3. Structural Data

Slip data from fault planes observed in the trench walls were measured for defining the kinematic properties of Orhaneli Fault. Generally kinematic markers such as slickenlines or groove marks were preserved in soft sediments like clay and silt on the fault planes. These structures were clearly observed in Kusumlar and Serçeler trenches, and the slip data were measured (Figure 11 A and B). These data showed that the fault remained under the effect of continuous similar tectonic deformation for a long time. The method recommended by Marrett and Allmendinger (1990) involving FaultKinWin 7.0.0 [computer program developed by R.A. Almendinger et al. (2012) for analysis of fault plane data] was used for fault plane analyses and the results are presented as focal mechanism solutions (Figure 11C).

A total of 5 slip data were measured in the trenches were assessed within the FaultKinWin program. The Orhaneli Fault was found out to have been affected by NE-SE oriented compression and the fault has reverse/thrust fault character with very small right-lateral component (Figure 11C).

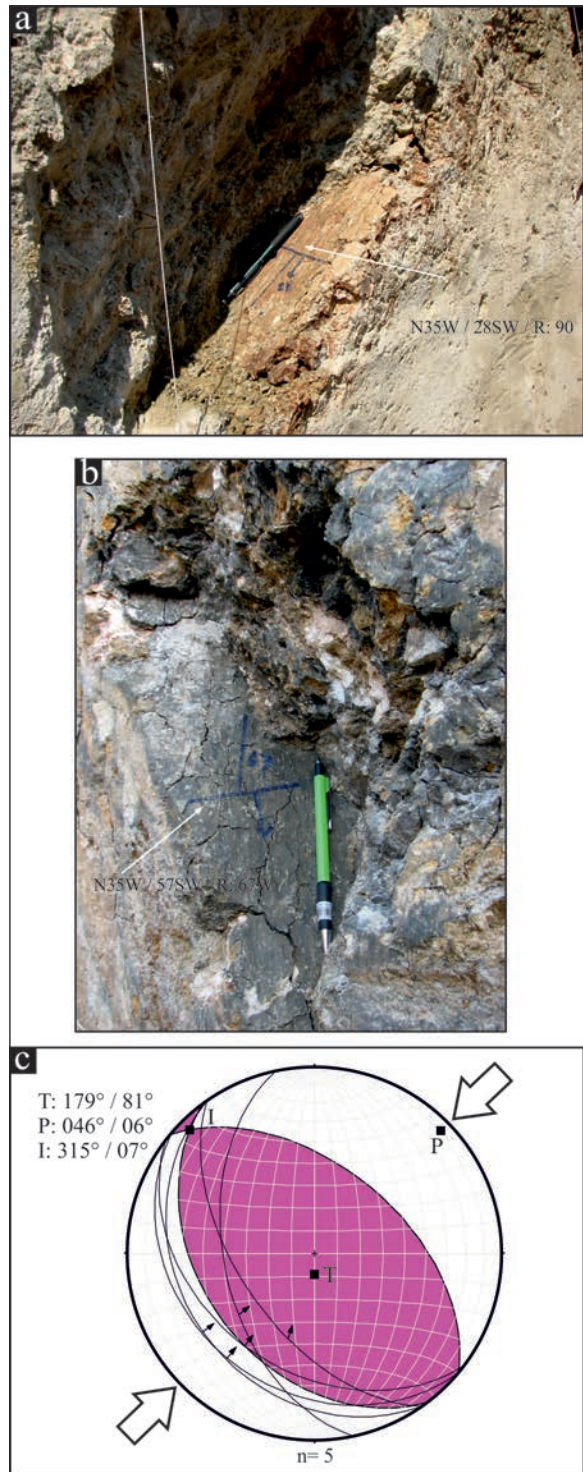


Figure 11- Photographs related to fault planes in A) Kusumlar Trench and B) Serçeler Trench. C) Data obtained from fault planes in the trenches displayed on an equal-area lower hemisphere (P: compression axis, T: extensional axis, I: intermediate axis). Fault plane solutions used the FaultKinWin V. 1.2.2. software (Marret and Allmendinger, 1990; Allmendinger et al., 2012).

6. Discussion and Conclusions

There are many active faults in the Biga Peninsula representing a transitional belt between the West Anatolian extensional tectonic regime and the North Anatolian Fault Zone (Barka, 1992; Barka and Kadinsky-Cade, 1988; Dewey and Şengör, 1979; Emre et al. 2012; 2013; Şaroglu et al., 1992; Şengör et al., 2005). These faults located in the region are generally right-lateral strike-slip faults, displaying an arc geometry widening toward the south (Figure 1B) (Emre et al., 2011a, b, 2013). The Orhaneli Fault forming the eastern wing of this arc was reported to be a right-lateral strike-slip fault by Emre et al. (2011a, 2012, 2013). Additionally, measurements on the fault planes during this study showed that the fault striations generally have rake angles between 70 to 80°; thus the NW segment of this fault basically has “reverse fault” character with very small amount of “right lateral strike-slip” component (Figure 11).

The fault planes observed in the trenches have general strike of N50°W, in accordance with the strike of the Orhaneli Fault on the Turkish Active Fault Map. During a palaeoseismology study of the Mustafakemalpaşa Fault, Kop et al. (2016) determined this fault had reverse slip component with right-lateral strike-slip character. This situation shows that the reverse component reduces and the right-lateral strike-slip component increases from Orhaneli Fault to Mustafakemalpaşa Fault in the northwest. Additionally, in the far northwest, the Manyas Fault representing the apex of the Manyas Bend nearly has “pure normal fault” character (Taymaz et al., 1991; Kürçer et al., 2017).

The stratigraphic and structural elements in Serçeler and Kusumlar trenches showed that four earthquakes were determined to have resulted in

surface ruptures in Quaternary. At least, two of them occurred in Holocene. Especially Kusumlar trench showed that the first Holocene earthquake occurred between. $6,600 \pm 1,200$ and $3,085-3,065$ BC (Figure 12; blue bar, earthquake no. 3), and the other earthquake occurred after 660-770 AD (Figure 12; blue bar, earthquake no. 1). In Serçeler trench the ante penultimate earthquake occurred between $22,000 \pm 3,200$ BC and $6,600 \pm 800$ BC (Figure 12; blue bar, earthquake no. 4) with the final earthquake observed to have occurred before 770 to 415 BC (Figure 12; blue bar, earthquake no. 2). According to palaeoseismologic results from Mustafakemalpaşa Fault located to the northwest, the oldest earthquake was before 2,190 BC (Figure 12; orange bar, earthquake no. 3) with the next earthquake between 815 BC and 1310 AD (Figure 12; orange bar, earthquake no. 2) and the final earthquake known to have occurred after 1425 AD (Figure 12; orange bar, earthquake no. 1) (Kop et al., 2016). The authors correlated the last event to the historical 1850 and 1851 earthquakes (Figure 12; orange bar, earthquake no. 1) and the penultimate event to the 368 AD earthquake (Figure 12; orange bar, earthquake no. 2). The last earthquake determined in this study may be related to the historical 1850 or 1851 earthquakes (Figure 12; blue bar, earthquake no. 1). If this possibility is correct, these earthquakes may have occurred due to the Orhaneli and Mustafakemalpaşa Faults together with each other. Kürçer et al. (2017) in addition to the last earthquake on the Manyas Fault in 1964 (Figure 12; yellow bar, earthquake no. 1) correlated the previous event to the 1323 AD earthquake (Figure 12; yellow bar, earthquake no. 2). When all these data are displayed on a timescale, it appears that there is a migration of earthquakes from the Orhaneli Fault toward the northwest, to the Mustafakemalpaşa and Manyas Faults, respectively (Figure 12). Here, no matter how broad the time interval is for the formation ages of some earthquakes, it is understood that there

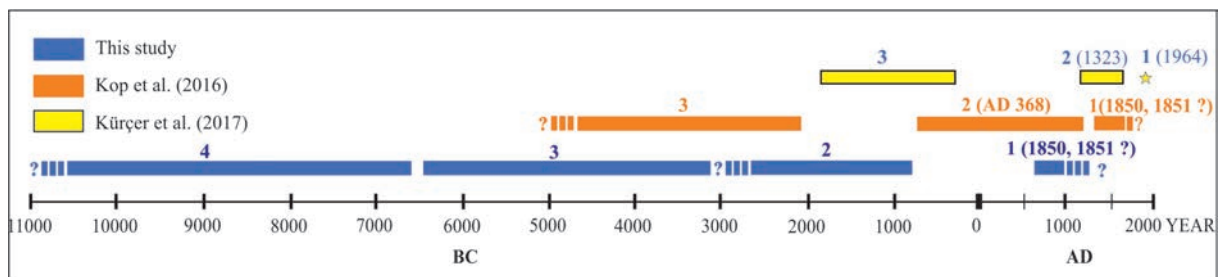


Figure 12- Palaeoseismological results for Orhaneli (this study), Mustafakemalpaşa (Kop et al., 2016) and Manyas (Kürçer et al., 2017) faults. Numbers are formation intervals for earthquakes, brackets refer to historical period earthquakes while yellow stars show instrumental period earthquakes.

is a large possibility that these earthquakes migrated from the SE (Orhaneli Fault) toward the NW (Manyas Fault).

There is similarity between the nearly 2.3 km right-lateral offset on the Orhaneli Stream (Figure 2) due to the fault, with the 2.5 km right-lateral offset of the same stream by the Mustafakemalpaşa Fault to the northwest (Emre et al., 2011b; Kop et al., 2016). According to this offset data from Orhaneli Stream, with drainage foundation known to be the Late Pliocene, the geologic slip rate of the Mustafakemalpaşa Fault was reported by Emre et al. (2011b) as 1 mm/yr, while Kop et al. (2016) suggested 0.7 mm/yr. In spite of the limited data availability, based on the offset caused by the Orhaneli Fault on the same streambed, the geologic slip rate may be proposed as 0.9-1 mm/yr. However, according to studies completed in the south Marmara Region in recent years, the incision ages of large valleys in the region are reported to be younger than 300.000 years (Kazancı et al., 2014). When this data is considered, the geologic slip rate may be recommended as 0.76 mm/yr.

Using data from this study and previous studies, it is not possible to make any interpretation of the recurrence interval for palaeo-earthquakes occurring in the region. However, according to calculations using the formula from Wells and Coppersmith (1994), if the Orhaneli Fault with total length of 30 km comprising two geometric segments fractured in a “single piece” it appears that it could produce an earthquake with magnitude M_w : 6.87. Similarly, Kop et al. (2016) stated that the Mustafakemalpaşa Fault could produce an earthquake with magnitude between M_w : 6.47 and 7.04.

In conclusion, for the first time activity twice in Holocene was determined for the Orhaneli Fault in this study. Rapidly increasing industrialisation and agricultural activities in the South Marmara Region have caused a rapid increase in population and the opening of new settlement areas. As a result, studies related to the active fault properties in the region gain great importance in terms of society. The data produced in this study will provide a significant contribution to earthquake risk analyses which are necessary for planning of all types of engineering structures and new settlement areas to be developed in the region currently and in the future.

Acknowledgements

This study was completed within the auspices of the “Turkish Palaeoseismology Research Project” led by the Directorate of Geological Studies of the General Directorate of Mineral Research and Exploration (Project Special Code No: 2013-30-14-07). We thank the reviewers Prof.Dr. Volkan Karabacak, Prof.Dr. Hasan Sözbilir, Prof.Dr. Levent Gülen and Dr. Hisao Kondo for their constructive criticism and contributions to the development of the manuscript.

References

- Allmendinger, R. W., Cardozo, N., Fisher, D. 2012. Structural geology algorithms: Vectors and tensors in structural geology (302 p.). Cambridge: Cambridge University Press.
- Ambraseys, N.N. 2002. The seismic activity of the Marmara Sea region over the last 2000 years. Bulletin of the Seismological Society of America, 92 (1), 1-18.
- Ambraseys, N.N., Finkel, C.F. 1991. Long term seismicity of İstanbul and of the Marmara region. Terra Nova 3, 527-539.
- Ambraseys, N.N., Jackson, J.A. 1998. Faulting associated with historical and recent earthquakes in the Eastern Mediterranean region. Geophysical Journal International 133, 390-406.
- Ambraseys, N.N., Jackson, J.A. 2000. Seismicity of the sea of Marmara (Turkey) since 1500. Geophysical Journal International 141, F1-F6.
- Barka, A.A. 1992. The North Anatolian Fault. Annales Tectonicae, 6, 164–195.
- Barka, A. A., Hancock, P. L. 1984. Neotectonic deformation patterns in the convex -northwards arc of the North Anatolian fault zone. In” The Geological Evolution of the Eastern Mediterranean region”, edited by J.E.Dixon and A.H.F.Robertson. Spec. Publ. Geol.Soc.London. 763-773.
- Barka, A.A., Kadinsky-Cade, K. 1988. Strike-slip fault geometry in Turkey and its influence on earthquake activity. Tectonics, 7, 663–684.
- Dewey, J.F., Şengör, A.M.C. 1979. Aegean and surrounding regions: Complex multiplate and continuum tectonics in a convergent zone. Geological Society of America Bulletin, 90, 84–92.
- Duman, T.Y., Çan, T., Emre, Ö., Kadirioğlu, F.T., Baştürk, N.B., Kılıç, T., Arslan, S., Özalp, S., Kartal, R.F., Kalafat, D., Karakaya, F., Azak, T.E., Özel, N.M., Ergintav, S., Akkar, S., Altınok, Y., Tekin, S., Cingöz, A., Kurt, A.İ. 2016. Seismotectonics

- database of Turkey. Bulletin of Earthquake Engineering, DOI 10.1007/s10518-016-9965-9
- Emre, Ö., Doğan, A., Özalp, S., Yıldırım, C. 2011a. 1:250.000 Scale Active Fault Map of Turkey Bandırma (NK 35-11b) Quadrangle. Maden Tetkik ve Arama 1:250.000 Scale Active Fault Map Series of Turkey, Serial No: 3, 55p., Ankara, Turkey (in Turkish) ISBN: 978-605-4075-86-4.
- Emre, Ö., Doğan, A., Özalp, S. 2011b. 1:250.000 Scale Active Fault Map of Turkey Balıkesir (NJ 35-3) Quadrangle. MTA 1:250.000 Scale Active Fault Map Series of Turkey, Serial No: 4, 35p., Ankara, Turkey (in Turkish).
- Emre, Ö., Doğan, A., Yıldırım, C. 2012. Biga Yarımadasının diri fayları ve deprem potansiyeli. In: Yüzer, E. and Tunay, G (Eds.), Biga Yarımadası'nın Genel ve Ekonomik Jeolojisi, General Directorate of Mineral Research and Exploration, Special Publication Series-28, 163-198, Ankara-Turkey (in Turkish).
- Emre, Ö., Duman, T.Y., Özalp, S., Elmacı, H., Olgun, Ş., Şaroğlu, F. 2013. Açıklamalı Türkiye Diri Fay Haritası. Ölçek 1:1.250.000, VI+89s.+bir pafta, Maden Tetkik ve Arama Genel Müdürlüğü, Özel Yayın Serisi-30, Ankara-Türkiye.
- Ergin, K., Güçlü, U., Uz, Z. 1967. A Catalog of Earthquakes for Turkey and Surrounding Area (11 A.D. to 1964 A.D.). Technical Report, İstanbul Technical University, Faculty of Mines, Institute of Physics of the Earth, No. 24, 169 p.
- Ergin, K., Güçlü, U., Aksay, G. 1971. A Catalog of Earthquakes of Turkey and Surrounding Area (1965-1970). Technical Report, İstanbul Technical University, Faculty of Mines, Institute of Physics of the Earth, no. 28.
- Harris, N.B.W., Kelley, S.P., Okay, A.I. 1994. Postcollision magmatism and tectonics in northwest Turkey. Contributions to Mineralogy and Petrology, 117, 241-252.
- Kadirioğlu, F.T., Kartal, R.F., Kılıç, T., Kalafat, D., Duman, T.Y., Eroğlu Azak, T., Özalp, S., Emre, Ö. 2016. An Improved Earthquake Catalogue ($M \geq 4.0$) for Turkey and Its Near Vicinity (1900-2012). Bulletin of Earthquake Engineering, (in press) doi: 10.1007/s10518-016-0064-8
- Kaya, O., Kozur, H., Sadeddin, W., Helvacı, H. 2001. Late Norian conodont age for a metacarbonate unit in NW Anatolia, Turkey. Geobios, 34, 527-532.
- Kazancı, N., Emre, Ö., Erturaç, K., Leroy, S., Öncel, S., İleri, Ö., Toprak, Ö. 2014. Güney Marmara Bölgesindeki Büyük Vadilerin Olası Deşilme Zamanı. Maden Tetkik ve Arama Dergisi, Sayı: 148, s: 1-17, Ankara, Türkiye.
- Konak, A. 2002. 1:500.000 Ölçekli Türkiye Jeoloji Haritası İzmir Paftası. Maden Tetkik ve Arama Genel Müdürlüğü, Ankara, Türkiye.
- Kondorskaya, N.V., Ulomov, V.I. 1999. Special catalogue of earthquakes of the Northern Eurasia (SECNE). URL: <http://socrates.wdcb.ru/scetac/> and <http://www.seismo.ethz.ch/gshap/neurasia/nordasiacat.txt>
- Kop, A., Özalp, S., Elmacı, H., Kara, M., Duman, T.Y. 2016. Active Tectonic and Paleoseismological Features of the Western Section of Mustafakemalpaşa Fault; Bursa, NW Anatolia. Geodinamica Acta, 28, 4, 363-378.
- Kürçer, A., Özaksoy, V., Özalp, S., Uygun-Güldoğan, Ç., Özdemir, E., Duman, T.Y. 2017. The Manyas Fault Zone (Southern Marmara Region, NW Turkey): Active Tectonics and Paleoseismology. Geodinamica Acta, 29, 1, 42-61.
- Marrett, R. A., Allmendinger, R. W. 1990. Kinematic analysis of fault-slip data. Journal of Structural Geology, 12, 973-986.
- McKenzie, D. 1972. Active tectonics of the Mediterranean region. Geophysical Journal of the Royal Astronomical Society, 30, 109-195.
- Okay, I.A. 1985. Kuzeybatı Anadolu'da yer alan metamorfik kuşaklar. Ketin Simpozyumu Kitabında, Türkiye Jeoloji Kurumu Yayını, 83-92.
- Okay, I.A. 2004. Tectonics and High Pressure Metamorphism in northwest Turkey. Field trip guide book - P01, 32nd International Geological Congress, APAT, Italy, 56 pp.
- Okay, I.A. 2011. Tavşanlı Zonu: Anatolid-Torid Bloku'nun Dalma-Batmaya Uğramış Kuzey Ucu. Maden Tetkik ve Arama Dergisi, Sayı: 142, Ankara.
- Okay, A.I., Tüysüz, O. 1999. Tethyan sutures of northern Turkey. In "The Mediterranean Basins: Tertiary extension within the Alpine orogen" (eds. B. Durand, L. Jolivet, F.Horváth ve M.Séranne), Geological Society of London, Special Publication 156.
- Okay, A.I., Harris, N.B.W., Kelley, S.P. 1998. Exhumation of blueschists along a Tethyan suture in northwest Turkey. Tectonophysics, 285, 275-299.
- Özalp, S., Emre, Ö., Doğan, A. 2013. Kuzey Anadolu Fayı Güney Kolu'nun segment yapısı ve Gemlik

- Fayı'nın paleosismik davranışı, KB Anadolu. Maden Tetkik ve Arama Dergisi, 147, 1-17, Ankara.
- Özalp, S., Kürçer, A., Özdemir, E., Duman, T.Y. 2016. The Bekten Fault: The paleoseismic behaviour and kinematic characteristics of an intervening segment of the North Anatolian Fault Zone, Southern Marmara Region, Turkey. *Geodinamica Acta*, 28, 4, 347-362.
- Reilinger, R., McClusky, S., Vernant, P., Lawrence, S., Ergintav, S., Cakmak, R., Ozener, H., Kadirov, F., Guliev, I., Stepanyan, R., Nadariya, M., Hahubia, G., Mahmoud, S., Sakr, K., ArRajehi, A., Paradissis, D., Al-Aydrus, A., Prilepin, M., Guseva, T., Evren, E., Dmitrova, A., Filikov, S.V., Gomez, F., Al-Ghazzi, R., Karam, G. 2006. GPS constraints on continental deformation in the Africa-Arabia-Eurasia continental collision zone and implications for the dynamics of plate interactions. *Journal of Geophysical Research*, 111, B05411.
- Servais, M. 1982. Collision et suture téthysienne en Anatolie Centrale, étude structurale et métamorphique (HP-BT) de la zone nord Kütahya. Ph.D. Thesis, Université de Paris-Sud, Centre d'Orsay, 374 s.
- Soysal, H., Sipahioğlu, S., Kolçak, D., Altınok, Y. 1981. Historical Earthquake Catalogue of Turkey and Surrounding Area (2100 B.C.–1900 A.D.). Technical Report, TÜBİTAK, Project No. TBAG-341, 87 p., İstanbul.
- Sözbilir, H., Özkaymak, Ç., Uzel, B., Sümer, Ö., Eski, S., Tepe, Ç. 2016a. Palaeoseismology of the Havran-Balıkesir Fault Zone: evidence for past earthquakes in the strike-slip-dominated contractional deformation along the southern branches of the North Anatolian fault in northwest Turkey. *Geodinamica Acta*, 28, 4, 254–272.
- Sözbilir, H., Sümer, Ö., Özkaymak, Ç., Uzel, B., Güler, T., Eski, S. 2016b. Kinematic analysis and palaeoseismology of the Edremit Fault Zone: evidence for past earthquakes in the southern branch of the North Anatolian Fault Zone, Biga Peninsula, NW Turkey. *Geodinamica Acta*, 28, 4, 273–294.
- Şaroğlu, F., Emre, Ö., Kuşçu, İ. 1992. Active Fault Map of Turkey. 1:1,000,000 Scale, General Directorate of Mineral Research and Exploration, Ankara-Turkey.
- Şengör, A.M.C., Görür, N., Şaroğlu, F. 1985. Strike-slip faulting and related basin formation in zones of tectonic escape: Turkey as a case study. In: Biddle, K.T. and Christie-Blick, N. (Eds.), *Strike-Slip Deformation, Basin Formation, and Sedimentation*, Spec. Publ. Soc. Econ. Paleontol. Mineral., 37, 227–264.
- Şengör, A.M.C., Tüysüz, O., İmren, C., Sakıncı, M., Eyidoğan, H., Görür, N., Le Pichon, X., Rangin, C. 2005. The North Anatolian Fault: A new look. *Annu. Rev. Earth Planet. Sci.*, 33, 37-112.
- Tan, O., Tapırdamaz, M.C., Yörük, A. 2008. The earthquake catalogues for Turkey. *Turk. J. Earth Sci.*, 17, 405-418.
- Taymaz, T., Jackson, J.A., McKenzie, D. 1991. Active tectonics of the North and Central Aegean Sea. *Geophysical Journal International*, 106, 433-490.
- Türkecan, A., Yurtsever, A. 2002. 1:500.000 Ölçekli Türkiye Jeoloji Haritası İstanbul Paftası. Maden Tetkik ve Arama Genel Müdürlüğü, Ankara, Türkiye.
- Wells, D., Coppersmith, K. 1994. New empirical relationships among magnitude, rupture length, rupture width, rupture area and surface displacement. *Bull. Seism. Soc. Am.*, 84, 974-1002.

